Rheological Behavior of Concentrated Silica Suspension and Its Application to Soft Armor

Tae Jin Kang, Chang Youn Kim, Kyung Hwa Hong

Intelligent Textile System Research Center, Seoul National University, Seoul 151-742, South Korea

Received 14 June 2010; accepted 6 May 2011
DOI 10.1002/app.34843
Published online 20 October 2011 in Wiley Online Library (wileyonlinelibrary.com).

ABSTRACT: The objective of this study is to develop an advanced stab and/or ballistic proof material composed of shear thickening fluid (STF) and Kevlar composite fabric. In this study, we prepared STF using sphere silica and fumed silica as silica particles and ethylene glycol and polyethylene glycol (PEG 200) as medium fluid, respectively. And the rheological properties of the STF were investigated under different conditions. Also, we impregnated Kevlar fabrics with the STF, and investigated the stab and ballistic resistances of the targets layered by the STF impregnated Kevlar fabrics. From the results, we observed that the STF significantly showed the reversible liquid–solid transition at a certain shear rate, and the STF treatment significantly improved the stab and ballistic resistance of Kevlar fabric. © 2011 Wiley Periodicals, Inc. J Appl Polym Sci 124: 1534–1541, 2012

Key words: shear thickening fluid (STF); fumed silica; sphere silica; Kevlar composite; stab resistance; ballistic resistance; liquid body armor

INTRODUCTION

Personal body armor is a protective covering used to prevent damages from being inflicted to an individual through direct contact weapons or projectiles usually during combat, or from a potentially dangerous environment or action.[1] Throughout recorded history, humans have used various types of materials to protect themselves from injury in combat and other dangerous situations. At first, protective coverings were made from animal skins. As civilizations became more advanced, wooden shields and then metal shields came into use. However, with the advent of firearms, most of the traditional protective devices were no longer effective.[2] Therefore, many scientists have tried to explore the possibility of using soft armor manufactured from various polymers. Of all the equipment developed and evaluated in the 1970s by National Institute of Justice (NIJ), one of the most significant achievements was the development of body armor, which employed DuPont's Kevlar® ballistic fabric comprised of para-aramid synthetic fiber. However, they are still heavy, bulky, and rigid because dozens of layers of Kevlar fabric are necessary to gain the certain level of stab- and/or bullet-proof performance. Thus, wearing the body armor made of the layers of Kevlar fabric may restrict the wearer's freedom of movement, and also it is impractical to use the material on the wearer's joints, arms, legs, neck, etc.[3] Therefore, recently the University of Delaware and the US Army are developing a new technology to save more soldiers' lives in combat.[4] This new technology is liquid body armor. The key component of the liquid armor is a shear thickening fluid (STF), a kind of concentrated hard particle suspension. STF shows flowable and deformable behavior under ordinary conditions. However, once a strong impact is applied, it turns rigid, showing a non-Newtonian flow behavior.[5] Hence, STF can be used as an aid material to improve the performance of the regular body armor made by Kevlar fabric. That is such a smart system which could allow the wearer flexibility for a normal range of movement, yet provide the armor with rigidity to resist piercing by bullets, stabbing knife blows, and similar attacks.[6,7]

Therefore, in this study we investigated the STF properties by the species of silica particle species and liquid medium to lay a basis for the preparation way of better performed liquid body armor. In addition, we prepared the STF/Kevlar composite fabrics, assessed them as stab- and/or bullet-proof materials, and then investigated their stab- and/or bullet-proof performances.

EXPERIMENTAL

Materials

Sphere silica and fumed silica (Aerosil 200) were obtained from Degussa Corporation (Akron, OH)

Correspondence to: K. H. Hong (hkh713@snu.ac.kr).
Contract grant sponsor: Korea Science and Engineering Foundation (KOSEF); contract grant number: R11-2005-065.

TABLE I
Specification of Sphere Silica and Fumed Silica

	Sphere silica	Fumed silica
Average particle size (nm)	120	300–400
Specific gravity (g/cm^3)	1.9	2.5
SiO_2-content (%)	90	99.8
pH (in 3 wt % dispersion)	5.43	3.7–4.7

and their properties are displayed in Table I. Kevlar fabric (plain weave, 28 × 28) was Kevlar-KM2 (600 denier) purchased from Barrday Inc. (Charlotte, NC). Ethylene glycol (EG) and polyethylene glycol (PEG 200) were purchased from Ducksan Pure Chemical Co. (Gyeonggi-do, Korea). All reagents were used as received without any further purification.

Preparation

Preparation of STF

To improve the dispersibility of silica particles in a medium fluid (EG or PEG), the silica particles were firstly pre-dispersed with a diluent (methanol), and then blended with the medium fluid. Subsequently, the dispersion was immediately treated by homogenization (via. IKA® T-25 Digital High-Speed Homogenizer Systems) for 1 h, and sonication for 10 h to further improve the dispersibility of the STF. Before investigating the rheological properties of the STF, we completely evaporated the methanol in STF in 65°C atmosphere.

Preparation of fumed silica/Kevlar composite fabrics

First, Kevlar fabrics were prepared by being each cut in size of 15 cm × 15 cm for stab resistance test and 7.5 cm × 7.5 cm for ballistic resistance test, based on the characterization standard and our preliminary test. The fabrics were immersed in as-prepared STF completely, and then the wet Kevlar fabrics were squeezed by a 2-roll mangle (applied pressure: 25 kg f/cm^2) to set a specific wet pick up (ca. 50%) and improve the STF infiltration into the Kevlar fabrics. Lastly, the fabrics were dried in a vacuum oven at 65°C for 24 h.

Characterization

The rheological properties of STF were investigated by a TA Instruments Rheometer-AR2000. The testing was carried out at a designed temperature in a steady-state flow mode and oscillation mode using a cone plate of size 40 mm and 2° angle. Stab resistance testing was carried out based on modified versions of NIJ standard 0115.00.[8] It was performed by mounting a NIJ standard spike in the crosshead of a load frame (Sintech 10/GL, MTS, Eden. Prairie, MN) with a 5 kN load cell, and monitoring the force inflicted on the load cell when the spike was driven into the fabric sample at a 15 mm/s speed. The fabric samples for the stab resistance test were prepared as a multiple layer form (8 layers) of identical Kevlar fabric. Ballistic resistance testing was performed by using a MIL-standard fragment simulation projectile (FSP), consisting of a chisel-pointed metal cylinder of 1.1 g and 0.56 cm diameter (22 caliber). The gun was sighted on the target center and the impact velocity was adjusted to approximately 250 m/s. A clay witness was made of Roma plastilina clay and used to measure the depth of indentation (modified NIJ standard-0101.04, 2001) (Fig. 1). The fabric samples for the ballistic resistance test were prepared as a multiple layer form (4 layers) of identical Kevlar fabric. In order to normalize the results with respect to variations in impact velocities, ballistic test results are also presented in terms of dissipated projectiles kinetic energy

$$E_d = 1/2 m_p \left(V_i^2 - V_r^2\right) \quad (1)$$

where E_d is the dissipated energy (J), m_p is the projectile mass (kg), V_i is the initial projectile velocity (m/s), and V_r is the residual velocity of the projectile after penetrating the target (m/s). In order to relate the depth of penetration to the residual projectile velocity, a series of experiments were performed using an empty target flame and clay witness.[9] The results showed that the penetration depth as a function of projectile velocity can be closely modeled by the linear relationship

$$V_r = 10.51 \times 2.43\, L \quad (2)$$

where L (m) is the penetration depth into the clay witness.[10] From eqs. (1) and (2), we obtained energy dissipation percentage (EDP) as follows;

$$\text{Energy dissipation } (\%) = (E_d/E_i) \times 100 \quad (3)$$

where E_i is the dissipated energy without target ($E_i = 1/2 \cdot m_p \cdot V_i^2$).

RESULTS AND DISCUSSION

Rheological properties of STFs

Effect of silica species and concentration

Fumed silica is a non-crystalline, fine-grain, low density, and high surface area silica prepared by a flame hydrolysis process.[11,12] The primary structure of the fumed silica consists of branch shaped aggregates (size: ca. 300–400 nm) formed by the fusion of primary spherical particles of SiO_2 (size: ca. 12 nm).

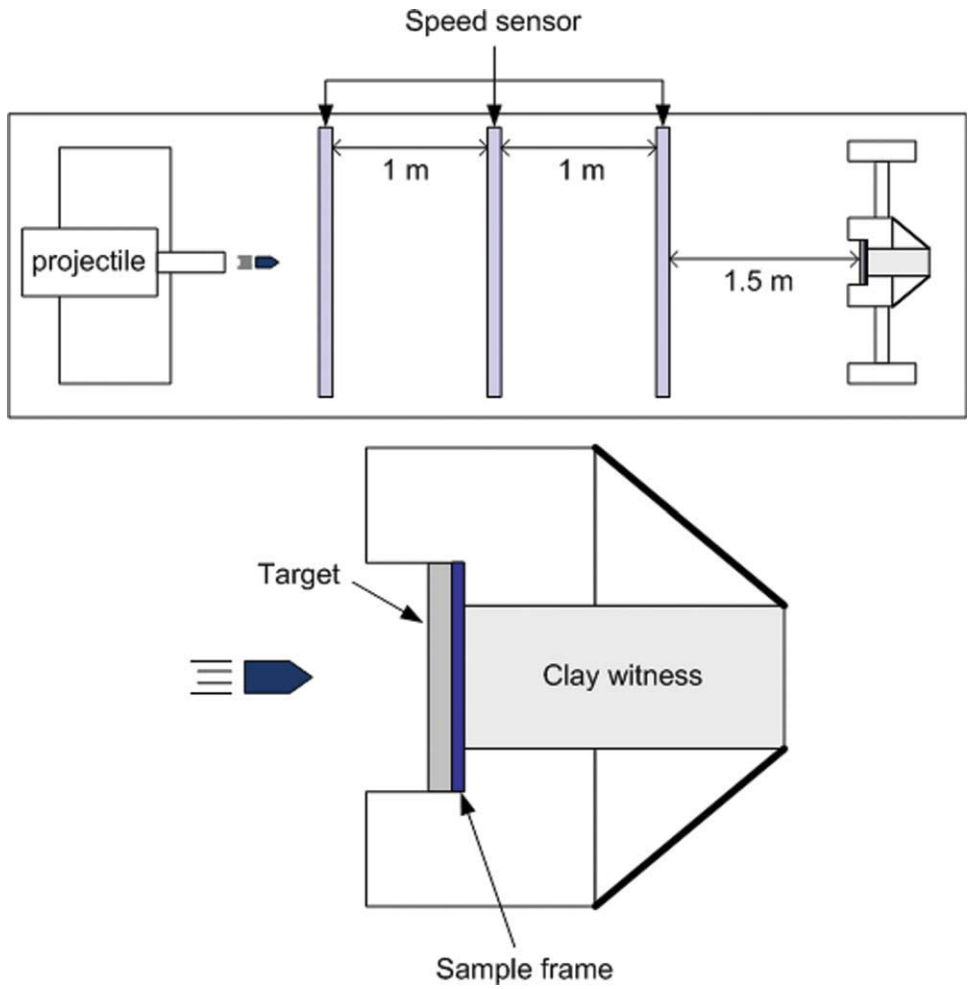

Figure 1 Schematic diagram of ballistic experimental setup. [Color figure can be viewed in the online issue, which is available at wileyonlinelibrary.com.]

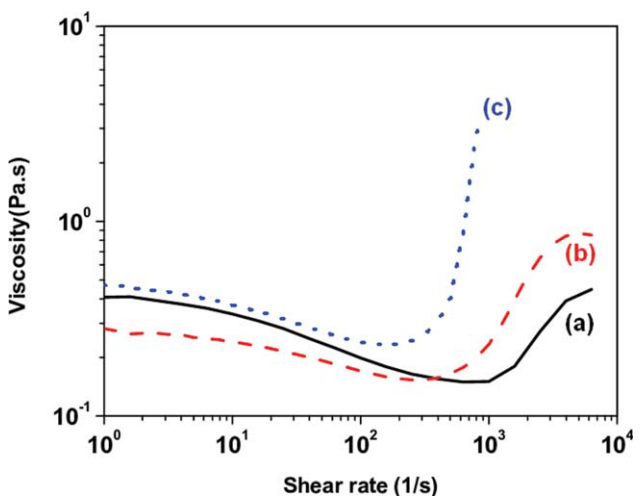

Figure 2 Steady-state viscosity curves for fumed silica/PEG suspension at various weight concentrations; (a) 20% fumed STF, (b) 25% fumed STF, (c) 27.5% fumed STF. [Color figure can be viewed in the online issue, which is available at wileyonlinelibrary.com.]

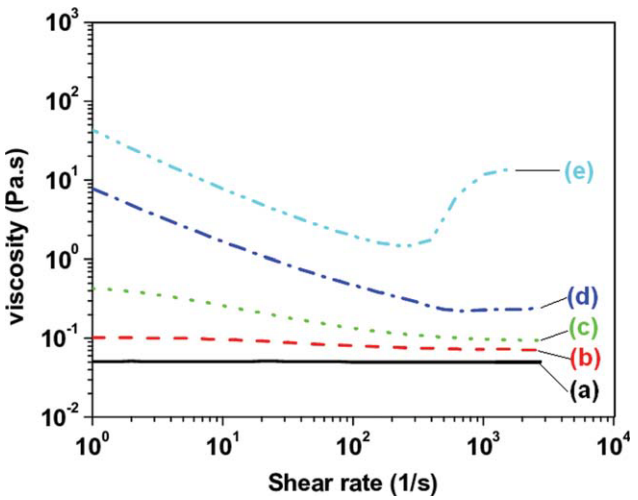

Figure 3 Steady-state viscosity curves for sphere silica/PEG suspension at various weight concentrations; (a) 5% STF, (b) 20% STF, (c) 35% STF, (d) 50% STF, (e) 65% STF. [Color figure can be viewed in the online issue, which is available at wileyonlinelibrary.com.]

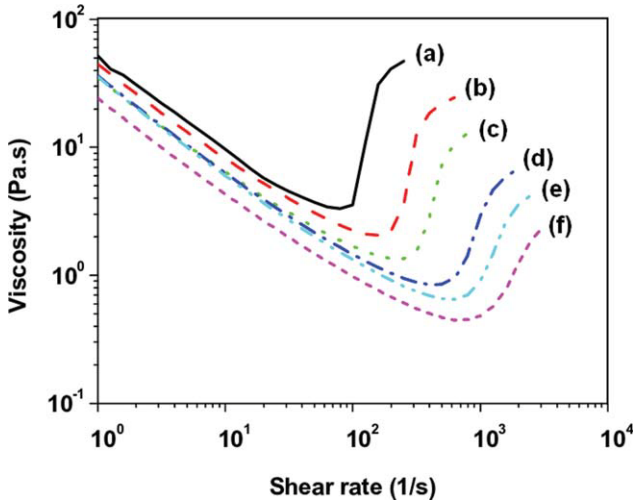

Figure 4 Steady-state viscosity curves for sphere silica/PEG suspension at various temperature (φ = 0.65); (a) 5°C, (b) 15°C, (c) 25°C, (d) 35°C, (e) 45°C, (f) 55°C. [Color figure can be viewed in the online issue, which is available at wileyonlinelibrary.com.]

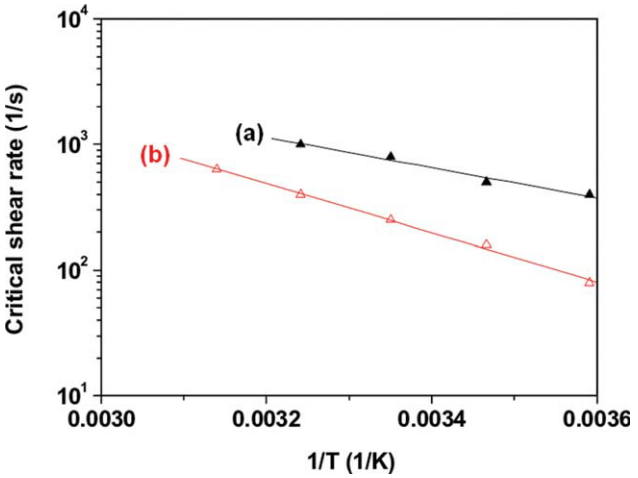

Figure 5 Temperature dependence of critical shear rate as a function of silica particle concentration; (a) sphere silica/PEG suspension (φ = 0.5), (b) sphere silica/PEG suspension (φ = 0.65). [Color figure can be viewed in the online issue, which is available at wileyonlinelibrary.com.]

Whereas, sphere silica (size: ca. 100–150 nm) does not form aggregates. Hence, the branch-shaped aggregates made up of fumed silica lead to a large increase in the viscosity of its STF and show gel-like behavior.[13] Therefore, the formation of hydrocluster[14–19] easily happened at low shear rates in the STF consisting of fumed silica rather than in the STF consisting of sphere silica, as shown in Figures 2 and 3. On the other hand, the critical shear rates of both STFs consisting of fumed silica and sphere silica appeared at lower shear rates as the concentrations of silica particle increased. And, the shear thickening phenomenon also happened further sharply with increasing the silica particle concentration. It seems that as silica particle concentration increased, the interparticle forces increased and so the friction between particles greatly increased, causing an enhanced shear thickening property of the STFs.[20]

Effect of temperature

We also observed that the critical shear rate and viscosity of the STF were varied by changing the temperature, as shown in Figure 4. This is because as temperature increased, the thermal Brownian motion of silica particles in liquid medium increased, and the hydrodynamic force inducing the dilatancy phenomenon also increased.[21] Also, Figure 5 shows that the dependence of critical shear rate on temperature grew with increasing the particle concentration, presumably due to the increased hydrodynamic interaction and interparticle forces in the STF.

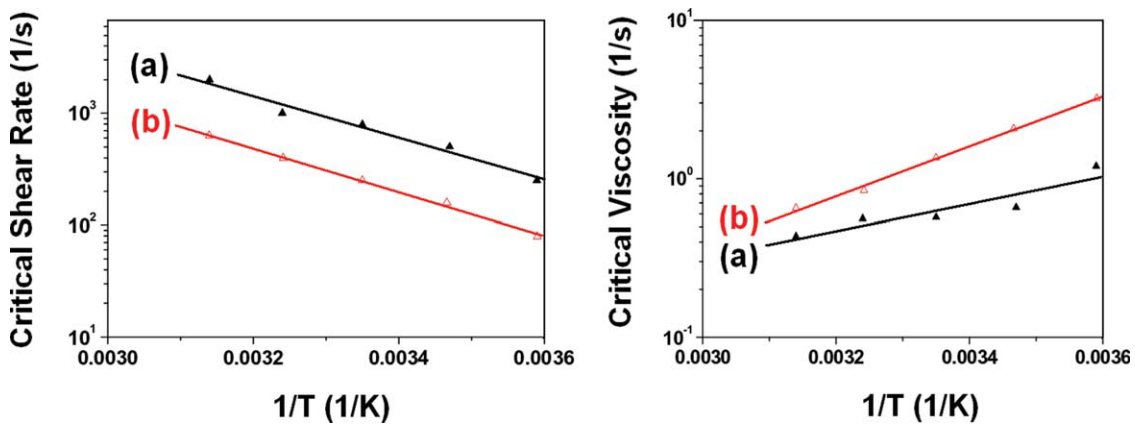

Figure 6 Temperature dependence of critical shear rate (left) and critical viscosity (right) as a function of liquid medium; (a) sphere silica/EG suspension (φ = 0.65), (b) sphere silica/PEG suspension (φ = 0.65). [Color figure can be viewed in the online issue, which is available at wileyonlinelibrary.com.]

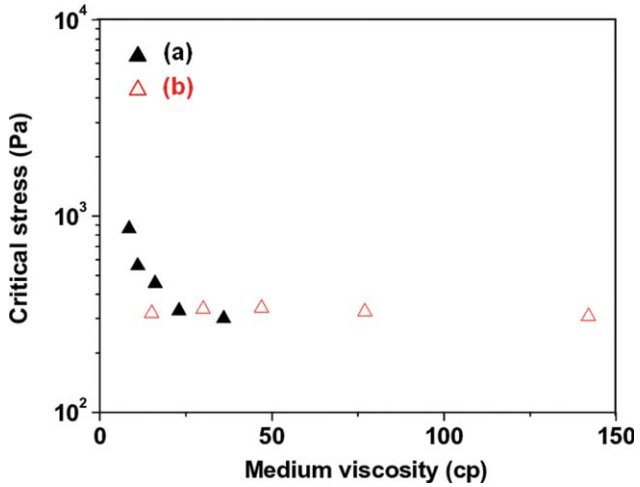

Figure 7 Critical stress for STF viscosity of sphere silica/EG suspension ($\varphi = 0.65$) (a) and sphere silica/PEG suspension ($\varphi = 0.65$) (b). [Color figure can be viewed in the online issue, which is available at wileyonlinelibrary.com.]

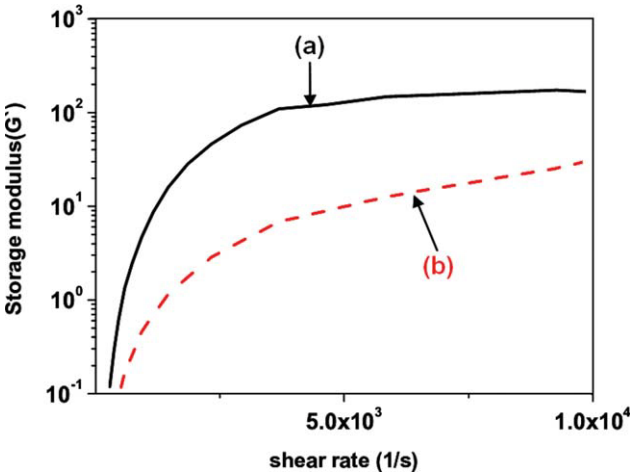

Figure 9 Storage modulus for shear rates of untreated sphere silica/PEG suspension (a) and plasma treated sphere silica/PEG suspension (b). [Color figure can be viewed in the online issue, which is available at wileyonlinelibrary.com.]

Effect of liquid medium

We investigated the effect of liquid medium of STF on the rheological properties in this study. Therefore, EG and PEG were used as the liquid medium. We found that the Peclet number of EG and PEG were similar (in range of 10^3–10^4), indicating both liquid media are comparable to each other in transport phenomena. Figure 6 shows that the critical shear rates (Fig. 6 (left)) and critical viscosities (Fig. 6 (right)) of both sphere silica/EG ($\varphi = 0.65$) and sphere silica/PEG ($\varphi = 0.65$) changed by varying the temperature of STFs. It was also observed that the critical shear rates of both STFs displayed the identical trend by temperature, but only showed the absolute difference between the STFs due to the difference of the viscosities between pure liquid media. However, the critical viscosity of sphere silica/PEG ($\varphi = 0.65$) further increased than that of sphere silica/EG ($\varphi = 0.65$) by temperature. On the other hand, we plotted the values of critical stress of both suspensions by effect of medium viscosity, as shown in Figure 7. From the results, we found that temperature influences the critical stress of STF not critical shear rate, and the interparticle forces in EG medium were more affected by temperature than those in PEG medium. It seems that the differences were from the naturally different heat diffusivities of the media; EG has high heat diffusivity whereas PEG has low heat diffusivity.[22,23]

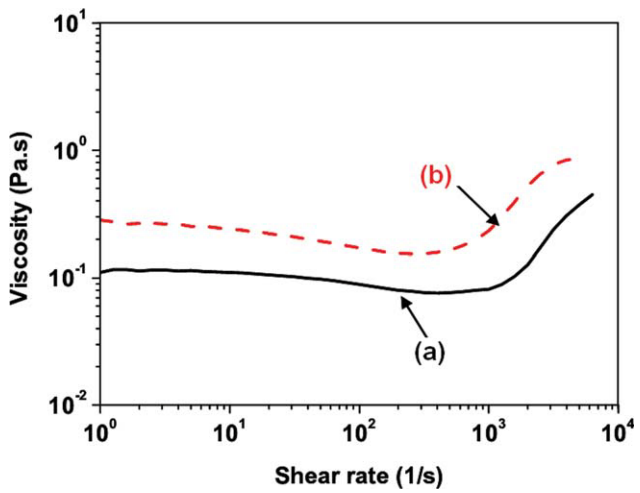

Figure 8 Steady-state viscosity curves of untreated sphere silica/PEG suspension (a) and plasma treated sphere silica/PEG suspension (b). [Color figure can be viewed in the online issue, which is available at wileyonlinelibrary.com.]

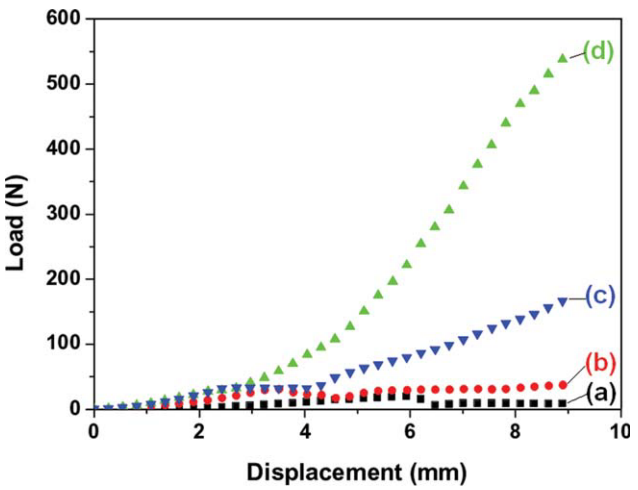

Figure 10 Load–displacements for quasistatic loading of neat Kevlar target (a), medium (EG) only treated Kevlar target (b), sphere silica particle treated Kevlar target (c), and sphere silica/EG suspension treated Kevlar target; target: 15 layers of each Kevlar fabrics. [Color figure can be viewed in the online issue, which is available at wileyonlinelibrary.com.]

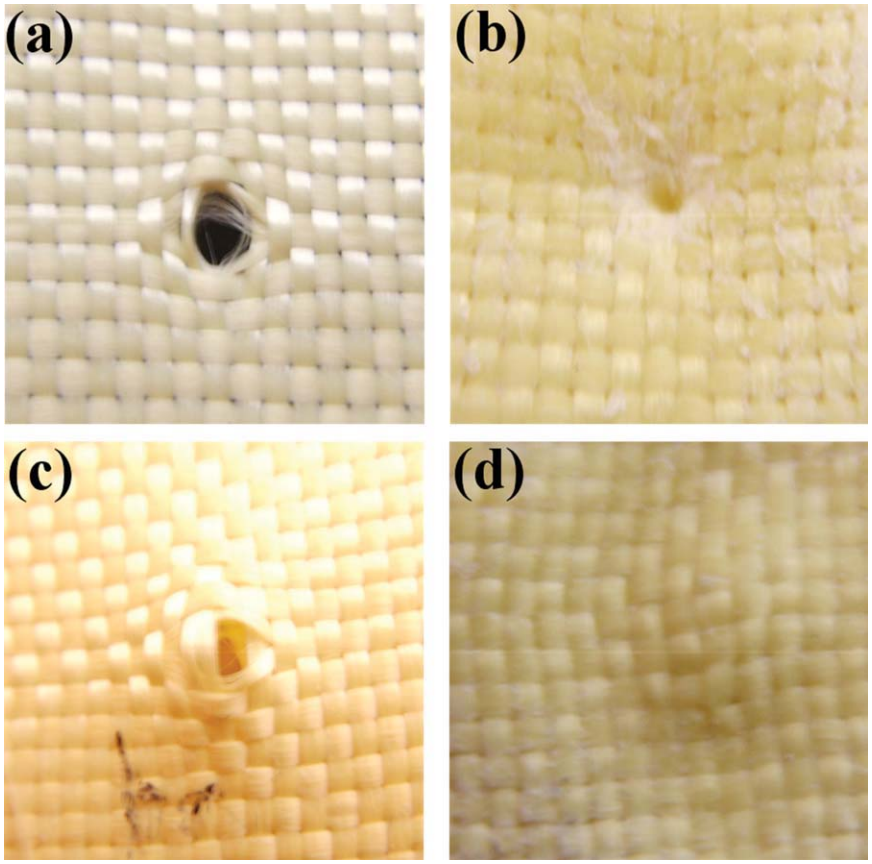

Figure 11 Photographs of neat Kevlar fabric and STF/Kevlar composite fabric after quasi-static stab testing; (a) neat Kevlar fabric_front, (b) neat Kevlar fabric_rear, (c) STF/Kevlar composite fabric_front, (d) STF/Kevlar composite fabric_rear. [Color figure can be viewed in the online issue, which is available at wileyonlinelibrary.com.]

Effect of plasma treatment

To improve the maximum volume fraction (φ_{max}) of fumed silica particle in medium fluid, we incorporate hydroxyl groups on the surface of the silica particles by plasma treatment (glow discharge method). As shown in Figure 8, plasma treated fumed silica suspension exhibited the shear thickening behavior at higher shear rate than untreated fumed silica suspension. Also the viscosity of plasma treated fumed silica suspension was lower than that of untreated fumed silica suspension. It seems that plasma treatment decreases the interparticle forces between fumed silica particles, and which induced deflocculation of the fumed silica suspension. On the other hand, Figure 9 shows that the plasma-treated fumed silica suspension absorbed more energy than untreated fumed silica suspension when the same amount of shear forces were inflicted on both STFs.

Features of STF/Kevlar composite fabrics

Stab resistant property

Figure 10 shows the quasi-static loading results for neat Kevlar, medium (EG) only treated Kevlar, sphere silica particle embedded Kevlar, and sphere silica/EG suspension treated Kevlar targets against the spike impactor threats. All targets consisted of 8 layers of each Kevlar fabrics. As seen in the graphs,

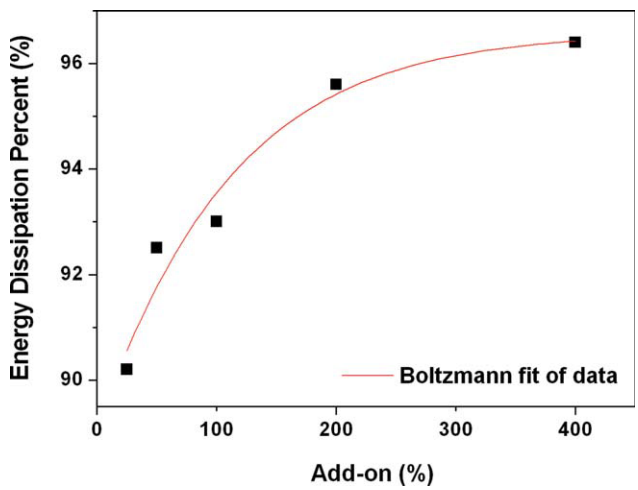

Figure 12 Energy dissipation percent of sphere silica/EG suspension treated Kevlar fabric targets as a function of add-on percent. [Color figure can be viewed in the online issue, which is available at wileyonlinelibrary.com.]

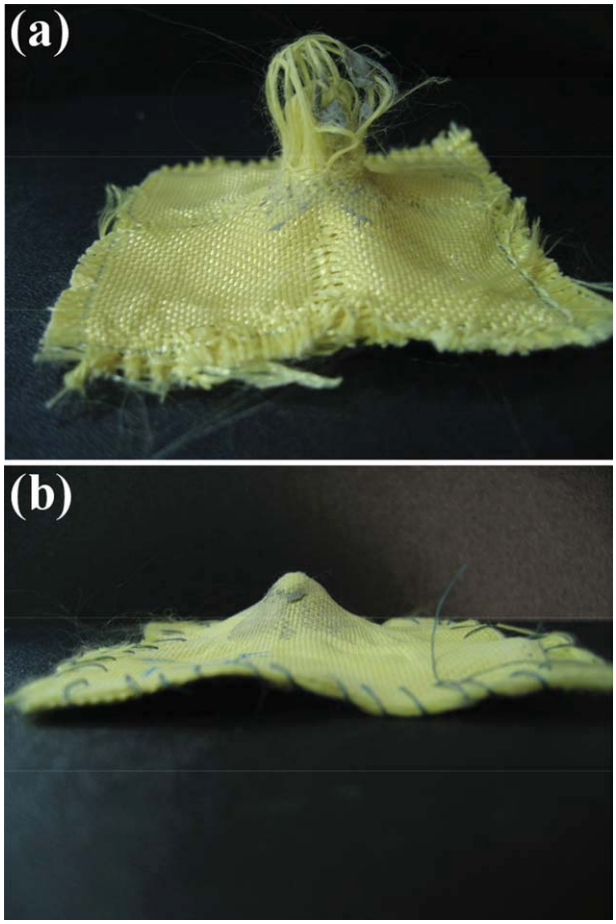

Figure 13 Photographs of neat Kevlar fabric (a) and sphere silica/EG suspension treated Kevlar composite fabric (b) after ballistic resistance testing. [Color figure can be viewed in the online issue, which is available at wileyonlinelibrary.com.]

sphere silica/EG suspension treated Kevlar target endured significantly higher load of about 550 N than neat Kevlar fabric target did of about 20 N. This result correlates with the appearance of the targets after the testing, the STF/Kevlar composite fabrics showed significantly less damage than neat Kevlar fabrics, as show in Figure 11. The results obviously show that the shear thickening behavior of STF was also revealed from sphere silica/EG suspension treated Kevlar fabrics. On the other hand, only the sphere silica powder embedded Kevlar target [Fig. 10(c)] also showed higher load than untreated Kevlar target. It was presumed that the applied silica powder raised the resistant force between the target and spike.

Ballistic resistant property

Figure 12 shows that the energy dissipation percent (EDP) of sphere silica/EG treated Kevlar targets (4 layers of the fabric) increased with increasing the add-on percent. It was thought that the higher add-on percent of STF induced more energy dissipation of the STF treated Kevlar fabrics, and thus the greater ballistic proof performance of the fabrics was achieved. This result correlates with the appearance of the targets after the ballistic resistance testing, as show in Figure 13.

CONCLUSION

This study reported the rheological properties of concentrated silica suspension, and the stab- and ballistic-resistance performance of the concentrated silica suspension treated Kevlar composite fabrics. The onset of shear thickening behavior shifted to higher shear rates with increasing the silica particle size, STF temperature, and STF stability. Also, the shear thickening behavior appeared at higher shear rates as volume fraction of the STF decreased. These phenomena seem to occur due to the Brownian motion, hydrodynamic force, and interparticle interaction. The effect of temperature on STF property clearly showed that the viscosity of STF and applied shear rate at critical transition point are on Arrehenius-type relation. Thus, their logarithmic values are inversely proportional to temperature, which means that the shear thickening behavior more readily enhances as temperature decreases. This is because the thermal Brownian motion weakens as temperature falls, which thereby prevents the particle rearrangement severely. On the other hand, STF impregnated Kevlar fabrics demonstrated a significant enhancement in stab and ballistic resistant properties due to the shear thickening properties of STF.

References

1. Wikipedia, ''Armour'', Ed. Ward Cunningham, http://en.wikipedia.org/wiki/Armor. Last accessed on: January 14, 2011.
2. Ashcroft, J.; Daniels, D. J.; Hart, S. V. Selection and Application Guide to Personal Body Armor, NIJ Guide 100–01 (Replaces Selection and Application Guide to Police Body Armor, NIJ Guide 100–98); The National Institute of Justice's National Law Enforcement and Corrections Technology Center, Rockville, MD, 2001.
3. Wilson, T. V. HowStuffWorks "How Liquid Body Armor Works," http://science.howstuffworks.com/liquid-body-armor.htm (2007). Last accessed on: January 14, 2011.
4. Wagner, N. J.; Brady, J. F. Phys Today 2009, 62, 27.
5. Barnes, H. A. J Rheol 1989, 33, 319.
6. Hassan, T. A.; Rangari, V. K.; Jeelani, S. Mater Sci Eng A 2010, 527, 2892.
7. Tonya, J. "Army Scientists, Engineers develop Liquid Body Armor," Military.com, (http://www.military.com/NewsContent/0,13319,usa3_042104.00.html) (2004). Last accessed on: March 4, 2011.
8. National Institute of Justice. Stab resistance of personal body armor. Standard 0115.000. Washington, DC: National Institute of Justice; 2000.

9. Lee, Y. S.; Wetzel, E. D.; Wagner, N. J. J Mater Sci 2003, 38, 2825.
10. Lee, Y. S.; Wetzel, E. D.; Egres, R. G., Jr.; Wagner, N. J. 23rd Army Science Conference, Olando, FL. Dec. 2–5, 2002. p 1.
11. Degussa Technical Bulletin No. 23, Degussa Corp., 1989.
12. Cabot Corp. Cab-o-sil Fumed Silica: Properties and Functions; Cabot Corp., Billerica, MA, 1987.
13. Khan, S. A.; Zoeller, N. J. J Rheol 1993, 37, 1225.
14. Bender, J. W.; Wagner, N. J. J Colloid Interface Sci 1995, 172, 171.
15. Bender J. W.; Wagner N. J Rheol 1996, 40, 899.
16. Phung, T. N.; Brady, J. F. J Fluid Mech 1996, 313, 181.
17. Melrose, J. R.; van Vilet, J. H.; Ball, R. C. Phys Rev Lett 1996, 77, 4660.
18. Farr, R. S.; Melrose, J. R.; Ball, R. C. Phys Rev D 1997, 55, 7203.
19. Brady, J. F.; Bossis, G. Ann Rev Fluid Mech 1988, 20, 111.
20. Cheremisihoff, N. P., Ed. Encyclopedia of Fluid Mechanics: Rheology and Non-Newtonian Flows; Gulf Publishing Company: Houston, Texas, 1988.
21. Boersma, W. H.; Laven, J.; Stein, H. N. AiChE J 1990, 36, 321.
22. Wikipedia, ''Ethylene glycol'', Ed. Ward Cunningham (2011) http://en.wikipedia.org/wiki/Ethylene_glycol. Last accessed on: March 28, 2011.
23. Wikipedia, ''Polyethylene glycol'', Ed. Ward Cunningham (2011) http://en.wikipedia.org/wiki/Polyethylene_glycol. Last accessed on: March 28, 2011.